Multiphoton ionization of cesium via quadrupole transitions: Photoelectron angular distributions and polarization effects on total ionization rates

A. Lyras,* Bonian Dai, X. Tang, and P. Lambropoulos*
Department of Physics, University of Southern California, Los Angeles, California 90089-0484

Adila Dodhy,† J. A. D. Stockdale, Dino Zei,‡ and R. N. Compton§
Chemical Physics Section, Health and Safety Research Division, Oak Ridge National Laboratory, Oak Ridge, Tennessee 37831-6125

(Received 23 December 1986; revised manuscript received 7 August 1987)

We report measurements of photoelectron angular distributions via electric quadrupole transitions in cesium atoms using multiphoton excitation techniques. Experimental results are presented for the cases of one-photon resonant, two-photon ionization via the $6d\,^2D_{3/2}$ and $6d\,^2D_{5/2}$ electric quadrupole transitions and for one-photon resonant, three-photon ionization via the $5d\,^2D_{3/2}$ and $5d\,^2D_{5/2}$ transitions. The ratios of the total ionization rates for linearly and circularly polarized light have also been measured for the $6d\,^2D_{3/2}$ and $6d\,^2D_{5/2}$ states. A theoretical analysis and detailed comparison with the experimental results are given.

I. INTRODUCTION

It has been shown theoretically[1] and verified experimentally[2] some time ago that with properly chosen resonance conditions, electric quadrupole transitions can dominate in multiphoton ionization (MPI). This offers the possibility of studying excited states which may otherwise be difficult to reach, thus providing spectroscopic information complementary to that obtained through dipole transitions.

After the early experiments[2] of this type on sodium, experimental[3] and theoretical[4–6] studies have concentrated on one-photon resonant, two-photon ionization in cesium atoms via the $6s\,^2S_{1/2}$ to the $6d\,^2D_{3/2,5/2}$ quadrupole transitions. Measurements with linearly and circularly polarized light were used to extract the ratios of the radial transition matrix elements from the $6d\,^2D_{3/2,5/2}$ levels to the p and f states (partial waves) of the continuum. In that experiment[3] the spin polarization of the photoelectrons was also measured, as it provides additional and, depending on the particular measurement, redundant information which is necessary for the extraction of atomic parameters. The overall agreement between experiment and theory[4–6] has, however, been poor, especially the ratio of two-photon ionization cross sections for linearly and circularly polarized light via resonance with the $6d\,^2D_{3/2}$ and $^2D_{5/2}$ states. The reasons for the disagreement so far have remained obscure.

In this work we undertake a complete analysis of the above resonant quadrupole MPI, including the possible effects of saturation, laser bandwidth, etc. Part of the motivation stems from the previous disagreement between the experimental results of Kaminsky *et al.*[3] and the calculations of Jaouen *et al.*,[4] who have reported ratios of generalized cross sections for linearly and circularly polarized light. Since for the case of exact resonance the amount of ionization is not simply proportional to a generalized cross section, it could not be expected *a priori* that experiment and the theory of Ref. 4 would agree even if both were correct. Resonance effects were not included in the formalism and calculations of Jaouen *et al.*[4]

Our aim in this paper is to assess these effects quantitatively through the comparison of new data with complete calculations in which all atomic parameters are obtained *a priori* through quantum-defect theory. The only experimental input has consisted of the laser power, bandwidth, and pulse duration. In cases of uncertainty, we have reported calculations for a range of values of the appropriate parameter (the laser power, for example) and examined the sensitivity of the results to such values. We find that the sensitivity may change dramatically in different ranges of intensity which can serve as a guide for the determination of an optimum intensity. Although the experimental data are in general agreement with theory, some remaining discrepancies underscore the usefulness of such measurements in the determination of atomic parameters.

Additional information about atomic structure is obtained through the study of photoelectron angular distributions (PAD), which in this case reflect the properties of the quadrupole-excited states. With the exception of two recent short papers,[7] very little work on PAD involving quadrupole transitions has been published. Although some of the information about such states can be obtained in principle without the involvement of quadrupole transitions, the latter provide the means for studying effects not easily accessible otherwise.

Although it was not our intention to elaborate on resonance line shapes in this publication, we do present a brief analysis of one example related to some of the transitions of interest in this paper. This example serves the twofold purpose of providing an additional consistency

test for our calculations and of illustrating certain features of such line shapes.

II. EXPERIMENTAL

A. Atomic beam apparatus

Details of the experimental apparatus employed to conduct the PAD studies have been published elsewhere.[8] Briefly, it consisted of a frequency-tunable dye laser, the polarization optics, the vacuum chamber which contained the alkali-atomic beam assembly and electron energy analysis and detection system, and the data acquisition system.

The dye laser (Quanta Ray model PDL-1) was pumped by a ND:YAG (yttrium aluminum garnet) laser (Quanta Ray model DCR2A). The output light of the dye laser had a pulse duration of ≈ 6 ns and a bandwidth of $\approx 0.02-0.03$ nm. The linearly polarized output light of the dye laser was further purified by a Glan-air polarizer and the degree of polarization P was determined to be better than 0.99. The polarization vector of the laser light was rotated using a double-Fresnel rhomb. The dye laser beam entered the vacuum chamber through a Pyrex window (thickness is 0.25 in.) and was focused into the alkali-atomic beam in a crossed arrangement using a 35-mm focal length lens. The estimated laser power density per pulse was $\approx 10^8$ W/cm^2. The cesium beam was generated by a standard thermal source equipped with a multichannel hole array to collimate the beam. The atomic number density at the point of intersection with the laser was estimated to be $\approx 10^{12}$ atoms/cm^3. Space-charge effects were minimized by keeping the number density low and controlling the laser power.

Photoelectrons emitted perpendicular to the direction of propagation of the laser beam were sampled and energy analyzed by a 160° spherical sector electrostatic energy analyzer. The energy resolution of the analyzer in these studies was ≈ 0.2 eV at a photoelectron transmission energy of ≈ 18 eV. The angular resolution of the analyzer was estimated to be $\approx \pm 1.5°$.

The photoelectrons transmitted through the analyzer were detected by a dual channelplate charged-particle detector and the signal after amplification was fed into a gated boxcar integrator (Princeton Applied Research model 165).

The output signal of the boxcar integrator, which is proportional to the initial photoelectron signal, was plotted on an x-y recorder, either as a function of the laser excitation wavelength or as a function of the kinetic energy of the photoelectrons. Photoelectron angular distributions were obtained by recording the boxcar integrator output signal as a function of the angle θ for $0 \leq \theta \leq 180°$, where θ is the angle between the direction of detection of the photoelectrons and the direction of the electric vector of the laser light. Photoelectron angular distributions for electric quadrupole transitions have an additional dependence on angle ϕ (azimuthal angle), which is defined between the direction of detection of the photoelectrons and the direction of propagation of the laser beam.[8] For all the measurements reported here $\phi \simeq \pi/2$. However, we note that the entrance axis of the photoelectron spectrometer is strictly oriented at right angles to the direction of propagation of the laser beam before it passes through the focusing lens. The actual azimuthal acceptance angle $\Delta\phi$ will therefore depend upon the focal length of the lens and the cross-sectional area of the laser beam. An axial ray through the lens will remain at a right angle to the acceptance axis of the analyzer. The marginal rays will introduce a change in the azimuthal acceptance angle ϕ of magnitude approximately a/f, where a is the diameter of the beam and f is the focal length of the lens. For our system this maximum change is $\approx 3°$. This is not expected to cause a significant change in the results reported here.

B. Heat-pipe apparatus

Measurements of the ratios of the ionization rates for linear and circularly polarized light were carried out not in a beam but by using a 38-cm active length cylindrical stainless steel "heat pipe" equipped with Pyrex windows (see Hamadani *et al.*[9]). The windows were found not to affect the polarization of the laser beam. The heat pipe was operated at room temperature or at low temperature ($< 50\,°$C) and without a buffer gas or at a very low buffer-gas pressure ($\ll 1$ Torr). Thus the apparatus was not operated in the heat-pipe mode. The pipe was equipped with a parallel off-center collecting wire which was biased several volts negative in order to collect the saturated positive-ion pulse produced by the unfocused collinear laser beam. The pulse was sampled by a fast digital oscilloscope (LeCroy 9400). This data-acquisition system allowed for immediate determination of the total charge collected for each laser pulse. The average of many such pulses was obtained. Circularly polarized light ($> 99\%$) was produced by a Soleil-Babinet compensator which was adjusted for each fine-structure state. Use of the compensator permitted changes from linearly to circularly polarized light without intensity or beam position changes. The laser beam intensity employed for both linearly and circularly polarized light was 2.0×10^5 W/cm^2. The entire voltage pulse was integrated to obtain the values used to calculate the circular to linear ionization ratios. Use of a long heat pipe allows for sensitive measurements of MPI without focusing the laser beam (low power density).

III. THEORY

The calculations of the reported angular distributions have been performed in the framework of perturbation theory of the appropriate order.[1,11] The interaction between light and electrons can be written in terms of the multipole expansion

$$V = V^D + V^Q + \cdots = -e\mathbf{r}\times\boldsymbol{\varepsilon}(0) - \tfrac{1}{2}e\sum_{i,j} Q_{ij}\nabla_j \varepsilon_i(0) + \cdots , \quad (1)$$

where only the electric dipole (V^D) and quadrupole (V^Q) terms have been retained. The quadrupole dyadic is defined by

$$Q_{ij}=x_i x_j-\tfrac{1}{3}r^2\delta_{ij},\quad i,j=1,2,3 \tag{2}$$

where $x_1=x$, $x_2=y$, $x_3=z$, and δ_{ij} is the Kronecker δ. $\varepsilon(0)$ is the electric field vector evaluated at the origin of the coordinates. For linearly polarized light we take z along the polarization direction and x along the propagation direction. Thus, only the $(\partial/\partial x)\varepsilon_z$ derivative is nonzero and equal to $ikzx$ for a field $\varepsilon_z e^{ikx}$. To within a multiplication factor the PAD is proportional to $|M_{fg}^{(N)}|^2$, where N is the order of the process (number of photons absorbed). For a two-photon quadrupole-dipole (QD) transition, we have

$$|M_{fg}^{(2)}|^2=\frac{\langle f|\mathbf{D}|\alpha_1\rangle\langle\alpha_1|\mathbf{Q}|g\rangle}{\omega_{\alpha_1}-\omega_g-\omega+\frac{i}{2}\Gamma_{\alpha_1}}\ , \tag{3a}$$

while for a three-photon quadrupole–dipole-dipole (QDD) transition we have

$$|M_{fg}^{(3)}|^2=\sum_{\alpha_2}\frac{\langle f|\mathbf{D}|\alpha_2\rangle\langle\alpha_2|\mathbf{D}|\alpha_1\rangle\langle\alpha_1|\mathbf{Q}|g\rangle}{(\omega_{\alpha_2}-\omega_g-2\omega)(\omega_{\alpha_1}-\omega_g-\omega+\frac{i}{2}\Gamma_{\alpha_1})}\ , \tag{3b}$$

where $|\alpha_1\rangle$ is the resonant intermediate state reached via the quadrupole transition and Γ_{α_1} its width, whose value does not matter in the angular distribution, as it factors out. The energies of the ground and intermediate atomic states are denoted by $\hbar\omega_g$, $\hbar\omega_{\alpha_1}$, and $\hbar\omega_{\alpha_2}$, respectively, while ω is the frequency of the incident photons. Apart from multiplication constants, the dipole and quadrupole operators are given by

$$\mathbf{D}=z\ , \tag{4a}$$

$$\mathbf{Q}=zx=\frac{1}{2}\left[\frac{8\pi}{15}\right]^{1/2}r^2(Y_{2,-1}-Y_{21})\ , \tag{4b}$$

where Y_{lm} are spherical harmonics. Since no spin analysis is performed, we must sum incoherently over the spin projection (along the laser polarization axis) of the outgoing electrons. We also average over the two magnetic substates of the ground state since under the conditions of the experiment the initial state is not aligned.

Specifically for the case of one-photon resonance with the $6\,^2D_j$ states, one has to calculate transition amplitudes of the form

$$M_{\pm1/2}^{\mu}\equiv\sum_{j'}\sum_{m_{j'}}\sum_{L,M_L}\alpha_{LM_L}^{*}(jm_j|LM_L s\mu)\times\langle K;Lsjm_j|\mathbf{D}|6;2\tfrac{1}{2}j'm_{j'}\rangle\times\langle 6;2\tfrac{1}{2}j'm_{j'}|\mathbf{Q}|6;0\tfrac{1}{2}\tfrac{1}{2},\pm\tfrac{1}{2}\rangle\ , \tag{5}$$

where the subscript refers to the initial-state magnetic number and the superscript $\mu=\pm\frac{1}{2}$ to the spin projection of the outgoing electron. The coefficients $\alpha_{LM_L}\equiv 4\pi^L e^{-i\delta_L}Y_{LM_L}^{*}(\theta,\phi)$, where δ_L is the phase shift of the Lth partial wave and (θ,ϕ) determine the direction of the outgoing electron. The final expression for the angular distribution is

$$f(\theta,\phi)=|M_{1/2}^{1/2}|^2+|M_{1/2}^{-1/2}|^2+|M_{-1/2}^{1/2}|^2+|M_{-1/2}^{-1/2}|^2\ . \tag{6}$$

A long and tedious calculation yields the following expressions for $f_{3/2}^{(2)}(\theta,\phi)$ and $f_{5/2}^{(2)}(\theta,\phi)$ corresponding to one-photon resonant, two-photon ionization through the $6D_{3/2}$ and $6D_{5/2}$ intermediate states, respectively:

$$f_{3/2}^{(2)}(\theta,\phi)=1+\beta_2\cos^2\theta+\beta_4\cos^4\theta\ , \tag{7}$$

where

$$\beta_2=-\frac{(7-3y^2+4y\cos\delta)+(12-3y^2-16y\cos\delta)\cos^2\phi}{(1+y^2+2y\cos\delta)(1+3\cos^2\phi)} \tag{8}$$

and

$$\beta_4=\frac{5(3-2y\cos\delta)}{(1+y^2+2y\cos\delta)}\left[\frac{1-\cos^2\phi}{1+3\cos^2\phi}\right], \tag{9}$$

with $\delta=\delta_1-\delta_3$ being the difference of the phase shifts of the p and f partial waves of the final continuum state and

$$y\equiv\frac{\langle\varepsilon p|r|6d|\rangle}{\langle\varepsilon f|r|6d\rangle}$$

the ratio of the two bound-continuum matrix elements contributing to the process. No j dependence of these matrix elements or phase shifts seems necessary in this case, as far as the angular distributions are concerned.

For $f_{5/2}$, we have

$$f_{5/2}^{(2)}(\theta,\phi)=1+\beta_2\cos^2\theta+\beta_4\cos^4\theta+\beta_6\cos^6\theta\ , \tag{10}$$

where

$$\beta_2=-\frac{(7+4y\cos\delta-3y^2)+(43+76y\cos\delta+8y^2)\cos^2\phi}{(1+2y\cos\delta+y^2)(1+8\cos^2\phi)}\ , \tag{11}$$

$$\beta_4=-\frac{5(2-2y\cos\delta)+20(8+3y\cos\delta)\cos^2\phi}{(1+2y\cos\delta+y^2)(1+8\cos^2\phi)}\ , \tag{12}$$

$$\beta_6=-\frac{125\cos^2\phi}{(1+2y\cos\delta+y^2)(1+8\cos^2\phi)}\ . \tag{13}$$

The most striking difference of these expressions from similar expressions of angular distributions through dipole transitions is their dependence on the azimuthal angle ϕ. The presence of the quadrupole transition breaks the cylindrical symmetry of the usual dipole transitions.

We note also that $f_{3/2}$ does not contain a $\cos^6\theta$ term because the anisotropy created by the intermediate state does not allow it since its total angular momentum is only $\frac{3}{2}$. On the contrary, the $\cos^6\theta$ term is, in general, present in the $f^{(2)}_{5/2}$ distribution. It vanishes, however, when $\phi=\pi/2$, as is evident from Eq. (13). An additional feature appears in that case. Not only does the $\cos^6\theta$ term vanish, but $f^{(2)}_{5/2}$ becomes identical to $f^{(2)}_{3/2}$, as can be readily verified by inspection of Eqs. (8)–(13). Basically, this is an interference effect, not in θ, which is the usual situation with angular distributions, but in ϕ. We encounter a more dramatic interference effect below, in connection with three-photon ionization.

For the one-photon resonant, three-photon ionization through the $5\,^2D_{3/2,5/2}$ intermediate states, the analytical results are extremely lengthy and will not be shown here. The distribution now has the form

$$f^{(3)}(\theta,\phi)=1+\beta_2\cos^2\theta+\beta_4\cos^4\theta+\beta_6\cos^6\theta+\beta_8\cos^8\theta\ , \tag{14}$$

where the coefficients β_{2n} are again functions of the phase shifts $\delta_0,\delta_2,\delta_4$ of the ratios of the respective bound-continuum matrix elements, as well as $\cos\phi$. It should be noted that we now have three even partial waves ($l=0,2,4$) contributing to the process, in contrast to a pure dipole three-photon process where only two odd partial waves ($l=1,3$) would contribute. As in the previous case of $6\,^2D$, the angular distributions observed via either fine-structure level, $^2D_{5/2}$,$^2D_{3/2}$, become identical when $\phi=\pi/2$.

All calculations of matrix elements and phase shifts necessary for the coefficients β_{2n} reported in Secs. IV B and IV C have been performed using quantum-defect theory. The two-photon matrix element entering in the dipole-dipole transitions from $5\,^2D_{5/2,3/2}$ to the continuum has been calculated through the quantum-defect Green's-function technique for the infinite summation over intermediate states.

For many aspects of resonance multiphoton transitions, a calculation in terms of the density matrix is necessary. This is particularly important for line shapes, peak heights, etc., especially under conditions of severe saturation. Angular distributions are affected only when two nearby states are coupled through the interaction with the field, as has been shown elsewhere,[11,12] and also demonstrated by experimental results with the appropriate analysis in previous papers by some of us.[8] It turns out, however, that under the conditions of the present experiments, saturation does not influence the PAD, which can therefore be described in terms of Eqs. (3a) and (3b). When we come to the analysis of peak heights, on the other hand, the density matrix becomes necessary in order to cope with the vanishing denominators, the finite laser bandwidth, etc. Occasionally it is possible to employ a simpler resonance formalism in terms of the amplitudes of the Schrödinger equation. We found it necessary to employ the density matrix for the ratio of resonance ionization for circular to linear polarization but more convenient to calculate the line shapes of Fig. 6(b) through the amplitude formalism.

IV. COMPARISON OF THEORY AND EXPERIMENT

A. Circular to linear ionization ratios

The MPI scheme for one-photon resonant, two-photon ionization via the $6d\,^2D_{3/2}$ and $6d\,^2D_{5/2}$ quadrupole transitions is shown in Fig. 1. A typical spectrum of the photoelectron signal as a function of the laser excitation wavelength obtained over the spectral region, $441\leq\lambda\leq443$ nm, at an estimated laser power density of $\approx10^8$ W/cm^2 is shown in Fig. 2.

Unlike weak-field spectroscopy, the strengths of resonance transitions with relatively strong lasers are not determined simply by the statistical weights of the resonant levels. Saturation, laser bandwidth, and pulse duration are some of the parameters that enter in a rather complex system of density-matrix equations through which the peak heights are determined. Often the result is counterintuitive, in that known regularities of line strengths are reversed in a multiphoton spectrum. The results are, moreover, intensity dependent. An example of such behavior was predicted in one of our earlier publications,[8] in which we have demonstrated a rather delicate power dependence on the three-photon ionization cross section resonantly enhanced by the $6s\,^2S_{1/2}\rightarrow6p\,^2P_{1/2,3/2}$ transitions in cesium. We have a similar situation here when we study the ratio of total ionization for light circularly polarized to that for linearly polarized. The experimental results for the two different resonances $6\,^2D_{5/2}$ and $6\,^2D_{3/2}$ are shown in Fig. 3, together with the results of our calculation as a function of laser power. The effect of large power is evident. In the limit of large power these ratios tend to unity because all atoms are ionized independently of polarization. The ratio does not approach unity monotonically but exhibits significant oscillations within a range of intensities from 10^6 to $\sim10^8$ W/cm^2. The experimental data were obtained at an intensity ($\sim10^5$ W/cm^2) which lies well within the flat part of the theoretical

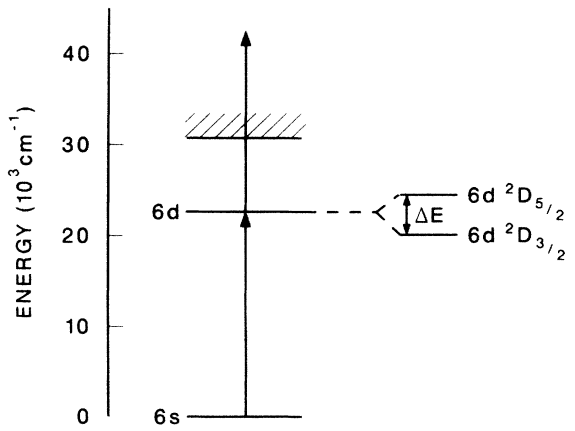

FIG. 1. Excitation scheme for one-photon resonant, two-photon ionization via the $6s\,^2S\rightarrow6d\,^2D_{3/2,5/2}$ quadrupole transitions in cesium atoms. The energy difference ΔE between the two fine-structure levels is 42.94 cm^{-1}.

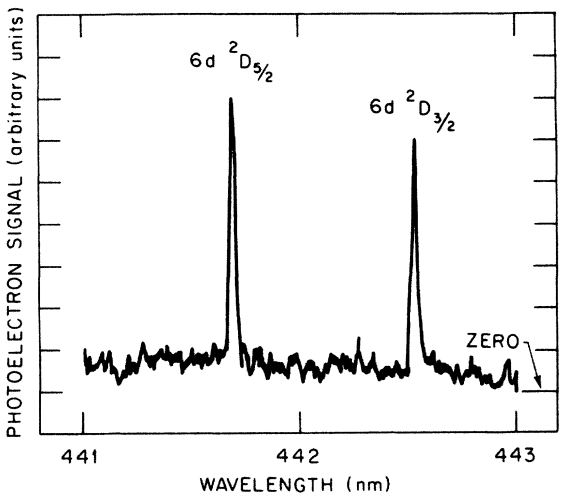

FIG. 2. Photoelectron signal as a function of the laser excitation wavelength for one-photon resonant, two-photon ionization via the $6s\,^2S_{1/2} \rightarrow 6d\,^2D_{3/2,5/2}$ quadrupole transitions in cesium atoms, for light linearly polarized.

values. We should therefore have the values 1.186 for the $6D_{5/2}$ resonance and 1.196 for the $6D_{3/2}$ resonance. The calculated value for $6D_{5/2}$ resonance is clearly outside the experimental error bars while for $6D_{3/2}$ resonance it is compatible with the lower value of the experimental error bracket.

To assess the possible reasons for this discrepancy, let us note first that in the low-intensity regime the ratio of the two-photon ionization cross section for circular to linear laser light for the $^2D_{3/2}$ intermediate can be written as

$$\rho_{3/2}=\frac{28R_F^2+2R_P^2}{22R_F^2+18R_P^2}=\frac{28+2y^2}{22+18y^2}\ , \tag{15}$$

while for the $^2D_{5/2}$ intermediate the ratio is

$$\rho_{5/2}=\frac{296R_F^2+14R_P^2}{234R_F^2+196R_P^2}=\frac{296+14y^2}{234+196y^2}\ , \tag{16}$$

where R_F and R_P are shorthand notations for the bound-continuum radial matrix elements $\langle \varepsilon f \mid r \mid 6d \rangle$ and $\langle \varepsilon p \mid r \mid 6d \rangle$, respectively, defined in Sec. III, together with the parameter $y=R_P/R_F$ appearing in Eqs. (11)–(13). The values of these parameters employed in our calculations have been obtained *a priori* (without input from the experiment) and lead to $y=0.29$, as obtained from single-channel quantum-defect theory. The value obtained by Jaouen *et al.*[4] for this parameter through a similar calculation, although slightly different from ours, is also compatible with the experimental value of $\rho_{3/2}$ at low intensity. Neither their values nor our values, however, are compatible with the experimental $\rho_{5/2}$. The experimental value of Kaminsky *et al.*[3] at a power density of $\sim 2\times 10^5$ W/cm^2 is $\sim 1.08\pm 0.04$ for the $6\,^2D_{3/2}$ resonance and 1.07 ± 0.03 for the $6\,^2D_{5/2}$ resonance.

From Eqs. (14) and (15), we see that the ratios ρ_j at-

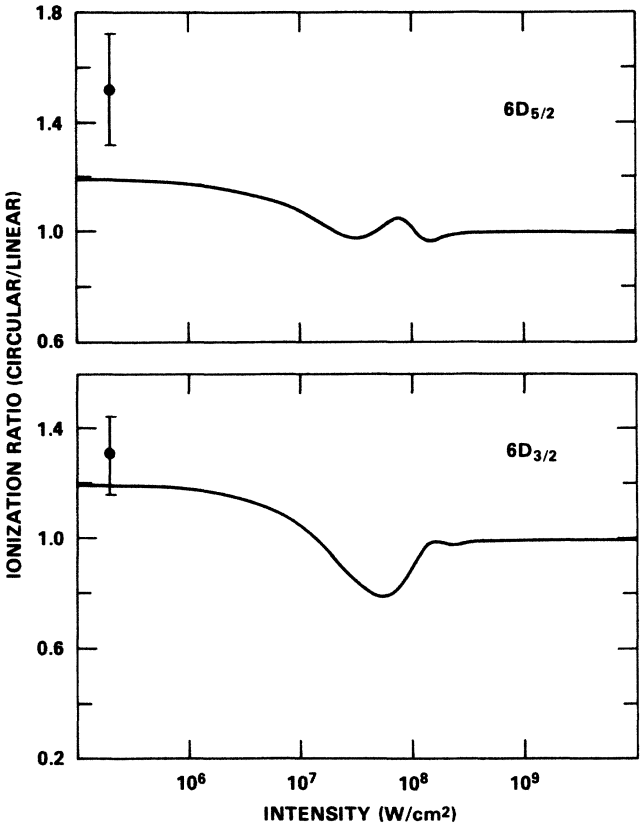

FIG. 3. The ratio of the total ionization rates (circularly to linearly polarized light) for one-photon resonant, two-photon ionization via the $6d\,^2D_{3/2} \leftarrow 6s\,^2S_{1/2}$ and $6d\,^2D_{5/2} \leftarrow 6s\,^2S_{1/2}$ electric quadrupole transitions in cesium as a function of laser power. The lines are the theory (see text), the points are the present experimental values. Limits shown are standard deviations.

tain their maximum value (in the low-intensity regime) for $y=0$, which in practice means $y \ll 1$. These maximum values are 1.273 for $\rho_{3.2}$ and 1.265 for $\rho_{5/2}$. Even in the limiting case, the theoretical result is outside the experimental error bars for $\rho_{5/2}$ but is compatible with the error bars for $\rho_{3/2}$. Although quantum-defect theory gave $y=0.29$, we cannot rule out the possibility that y is in fact smaller. Even $y=0.2$ would lead to a significant change of the ρ_j ratio while $y=0.1$ (which is entirely possible) would lead to values for ρ_j very close to their maxima. But still the discrepancy for $\rho_{5/2}$ cannot be removed no matter what the value of y may be. Moreover, laser intensity effects (even though there is no reason to doubt the low-intensity assumption) would make the discrepancy even worse.

In searching for other possible effects compatible with this discrepancy, we have considered the possibility of spin-orbit effects in the continuum. If such effects were present, they would cause the radial matrix elements from $6\,^2D_j$ to a continuum $\varepsilon l_{j'}$ to depend on j and j'. The expressions given in Eqs. (15) and (16) would no longer be valid in that case. We have carried out the relevant calculation, which is rather lengthy and need not be reproduced here. The resulting expressions are

$$\rho'_{3/2}=\frac{84+6(R_{P_{3/2}}/R_{F_{5/2}})^2}{66+4(R_{P_{3/2}}/R_{F_{5/2}})^2+5(R_{P_{3/2}}/R_{F_{5/2}})^2(R_{P_{1/2}}/R_{P_{3/2}})^2}\,, \tag{17}$$

$$\rho'_{5/2}=\frac{2000+72(R_{F_{5/2}}/R_{F_{7/2}})^2+98(R_{F_{5/2}}/R_{F_{7/2}})^2(R_{P_{3/2}}/R_{F_{5/2}})^2}{1600+38(R_{F_{5/2}}/R_{F_{7/2}})^2+1372(R_{F_{5/2}}/R_{F_{7/2}})^2(R_{P_{3/2}}/R_{F_{5/2}})}\,, \tag{18}$$

where the R's represent radial matrix elements from the respective states of the doublet $6D_{3/2,5/2}$ to the partial wave indicated by the subscripts of R. For example, $R_{F_{5/2}}$ in Eq. (17) stands for $\langle \varepsilon f(\frac{5}{2}) \mid r \mid 6d(\frac{3}{2})\rangle$, while $R_{F_{5/2}}$ in Eq. (18) stands for $\langle \varepsilon f(\frac{5}{2}) \mid r \mid 6d(\frac{5}{2})\rangle$, etc. Note first that the continuum $\varepsilon f(\frac{7}{2})$ does not enter at all in the ionization of the $6d_{3/2}$, owing to the dipole selection rules. All ratios of the form $R_{P_j}/R_{F_{j'}}$ in Eq. (17) will be of the order of 0.3 or less. Even if $R_{P_{1/2}}/R_{P_{3/2}}$ were as large as 20 or 30, the ratio $\rho'_{3/2}$ would not change much. The situation with $\rho'_{5/2}$ is entirely different. The ratio $R_{F_{5/2}}/R_{F_{7/2}}$ plays a crucial role in that case. A brief investigation of Eq. (18) shows that if, for example, the p-to-f partial-wave ratio is 0.1 while $R_{F_{5/2}}/R_{F_{7/2}}$ is of the order 10, the ratio $\rho'_{5/2}$ assumes the value 1.37, while $\rho'_{3/2}$ remains in the vicinity of 1.25.

There is quite a bit of uncertainty concerning spin-orbit effects in bound-continuum matrix elements from excited states such as the $6D$ state of cesium.[13] It is, on the other hand, known[14] that in the energy range around 4 eV above threshold, there are significant spin-orbit effects on matrix elements of the form $\langle \varepsilon p(\frac{3}{2},\frac{1}{2}) \mid r \mid 6S_{1/2}\rangle$ connecting the ground state with the continuum through single-photon absorption. In previous work[15] by some of us, indirect evidence has pointed to the possibility of similar effects in three-photon ionization from the ground state. All of the above, combined with the analysis based on Eqs. (17) and (18), support the conjecture that spin-orbit effects in the continuum may play a role. A systematic calculation of these effects represents a rather complex undertaking, which would be justifiable and of maximum utility if additional experimental data were available; it is a project which we intend to pursue in the near future.

To summarize the present status of this aspect, we are led to the tentative conclusion that the ratio of the p-to-f partial wave, namely y, may be smaller than the 0.29 given by quantum-defect theory, and that spin-orbit coupling in the continuum may introduce significant j dependence of the $\langle \varepsilon f j' \mid r \mid 6dj\rangle$ radial matrix elements.

B. Photoelectron angular distributions

1. $6d\ ^2D_{3/2,5/2}$ states

The results of the PAD measurements for the $6d\ ^2D_{3/2}$ and $6d\ ^2D_{5/2}$ states are shown by the solid dots in Figs. 4(a) and 4(b), respectively. It is interesting to note that the overall features of the two distributions are the same.

The β_{2i} coefficients [see Eq. (7)] were obtained from the experimental data by using a least-squares-fitting procedure and are presented in Table I. The coefficient β_0 has been normalized to unity.

From the β_{2i} coefficients in Table I, two noteworthy points can be seen. First, the best fit for both the $6d\ ^2D_{3/2}$ and $6d\ ^2D_{5/2}$ fine-structure states is given by a polynomial containing even powers of $\cos^{\alpha}\theta$ up to $\alpha=4$. In general, the PAD for the $6d\ ^2D_{5/2}$ state would be expected to contain the $\cos^6\theta$ term. Second, we note that the values of the β_{2i} coefficients for the two fine-structure states are similar, i.e., differences in the angular distributions for both fine-structure levels are experimentally undetectable. This is to be distinguished from angular distributions for two-photon resonant, three-photon ionization via $n\ ^2D_{5/2,3/2}$ states through dipole transitions, which are distinctly different.[8]

The β_{2i} coefficients obtained by using the theoretical analysis discussed earlier are shown in Table I, where β_0 has been normalized to unity. The PAD resulting from this analysis are shown by the solid lines in Fig. 4 and have been normalized to the experimental data at $\theta=0$.

From the theoretically calculated β_{2i} coefficients, it is seen that for $\phi=\pi/2$ the PAD for both the fine-structure states are described by a polynomial containing even powers of $\cos^{\alpha}\theta$ up to $\alpha=4$. It can also be seen that the β_{2i} coefficients for both cases are identical.

These theoretical results are consistent with the experimental observations. There remains, however, a discrepancy between the numerical values of the experimentally and theoretically determined β_{2i} coefficients. In order to understand this discrepancy let us consider the hyperfine coupling times $\tau_{\rm hfs}$ given by the inverse of the energy difference of the outer hyperfine structure levels, $F=2$ and $F=1$ and 6 for the $6d\ ^2D_{3/2}$ and $6d\ ^2D_{5/2}$ states. These times are ≈ 5.1 ns and ≈ 13.9 ns for the $6d\ ^2D_{3/2}$ and $6d\ ^2D_{5/2}$ states,[16] respectively, which are comparable to the 6-ns duration of the laser pulse. Thus, hyperfine coupling can occur during the ionization period, causing the initial alignment of the intermediate state to be partially lost and the PAD to be affected.[8] Exact theoretical estimates of hyperfine coupling effects in the present case would involve long and tedious labor. In view of our earlier work establishing the importance of these effects[8] and the reasonable qualitative agreement between experiment and the present theory, as shown in Fig. 4 and described above, we feel the present situation to be satisfactory.

2. $5d\ ^2D_{3/2,5/2}$ states

The MPI scheme for the one-photon resonant, three-photon ionization via the $5d\ ^2D_{3/2}$ and $5d\ ^2D_{5/2}$ quadru-

TABLE I. The β_i coefficients obtained by a least-squares-fitting procedure to the experimental data and by theoretical calculations for one-photon resonant, two-photon ionization via the $6d\ ^2D_{3/2,5/2}$ states and one-photon resonant, three-photon ionization via the $5d\ ^2D_{3/2,5/2}$ states of cesium atoms.

		Expt.			Theory			
State	β_0[a]	β_2	β_4	β_6	β_0	β_2	β_4	β_6
$6d\ ^2D_{3/2}$	1.00	−0.77±1.17	8.12±1.59		1.00	−8.26	20.42	
$6d\ ^2D_{5/2}$	1.00	−1.34±0.97	9.94±1.73		1.00	−8.26	20.42	
$5d\ ^2D_{3/2}$	1.00	2.18±1.95	1.36±4.18	4.34±3.18	1.00	−14.26	78.65	−14.30
$5d\ ^2D_{5/2}$	1.00	9.02±6.85	−3.34±11.07	8.84±8.81	1.00	−14.26	78.65	−14.30

[a]β_0 has been normalized to unity and the error associated with it is zero.

pole transitions is shown in Fig. 5. This case is rather unusual in that it is the first (to our knowledge) investigation of a quadrupole transition followed by two-photon ionization. In terms of transition strengths, this is equivalent to an overall four-photon purely dipole process.

The $5d\ ^2D_{3/2,5/2}$ doublet is in an energy region in which two-photon excitation to the $11s\ ^2S$ and $7f\ ^2F$ states are encountered as the photon frequency is varied from resonance with $5\ ^2D_{3/2}$ to resonance with the $5\ ^2D_{5/2}$, as shown in Fig. 6(a). The usual dipole-dipole two-photon transition is responsible for the resonance with the $11s$. The resonance with the $7f$ is, however, something unusual in that it involves a quadrupole-dipole (and dipole-quadrupole) two-photon transition without an intermediate single-photon resonance. It is, at first, surprising that the three resonances involving one quadrupole transition are equal to or higher than the purely dipole $11s$ resonance. The reason for this behavior has to do with the weakness of the two-photon dipole transitions to $11s$ as well as the weakness of photoionization from an excited s state. The spectrum, shown in Fig. 6(a), was obtained at a laser power of approximately 10^8 W/cm^2 and shows asymmetric profiles which are rather usual in this type of process. The chief cause of such profiles is Stark broadening originating from a slight but significant frequency dependence of the ac Stark shift of the resonance as the laser frequency is swept around it. The $5d\ ^2D_{3/2}$ resonance is Stark broadened towards the blue, while the $5d\ ^2D_{5/2}$ is Stark broadened toward the red. An important contribution to this behavior comes from the fact that when the energy of the first photon is varied around the $5d\ ^2D_{3/2}$ and $5d\ ^2D_{5/2}$ states, the second photon is in the vicinity of the $10p\ ^2P$ and $11p\ ^2P$ states, respectively. The nearby presence of the $7f\ ^2F$ state at the second-photon level also plays an important role, as does, of course, the general interference with the complete multiphoton background. A study of ac as well as dc Stark effects on MPI of cesium via the above four states has been presented by Klots and Compton.[10]

Given the above intricate interplay of quadrupole and resonance effects, we calculated these line shapes as an additional test of our theoretical model. Most critical is the correct prediction of peak heights, which, as mentioned earlier, turn out to be counterintuitive. The correct overall asymmetry is also important. We have been able to reproduce these features to a reasonable degree [see Fig. 6(b)] without using an input from the experiment other than the intensity, and also without any theoretical adjustable parameters. Under the conditions of these experiments, we find that a calculation in terms of amplitudes of the Schrödinger equation (rather than the density matrix) is sufficient. We are dealing in this case with a multilevel system whose complexity is increased by the participation of quadrupole transitions.

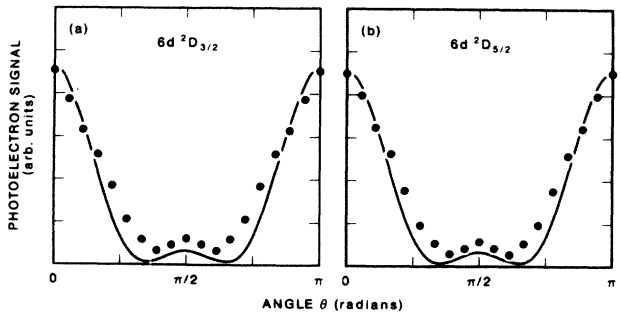

FIG. 4. Photoelectron angular distributions for one-photon resonant, two-photon ionization via the (a) $6s\ ^2S_{1/2} \rightarrow 6d\ ^2D_{3/2}$ and (b) $6s\ ^2S_{1/2} \rightarrow 6d\ ^2D_{5/2}$ quadrupole transitions in cesium atoms. The dots are the experimental values and the solid lines represent the theory. Standard deviations in the experimental values are approximately twice the diameter of the dots.

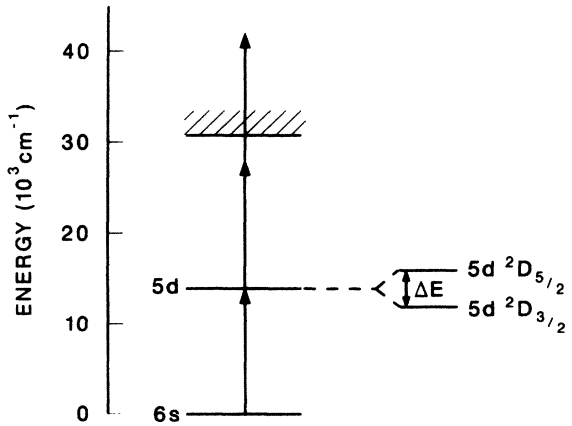

FIG. 5. Excitation scheme for one-photon resonant, three-photon ionization via the $6s\ ^2S_{1/2} \rightarrow 5d\ ^2D_{3/2,5/2}$ quadrupole transitions in cesium atoms. The energy difference ΔE between the two fine-structure levels is 97.59 cm^{-1}.

Because of such transitions, on the other hand, there is no saturation of the bound-bound transitions. As a result, the dominant width of the resonant states comes from ionization, which makes the treatment in terms of amplitudes adequate.

We turn now to the PAD measurements. Results for the $5d\,^2D_{3/2}$ and $5d\,^2D_{5/2}$ states are shown in Fig. 7. Theory predicts that these distributions should be independent of the fine structure of the D states and therefore identical. The overall features of the experimental distributions are indeed very similar. The β_{2i} coefficients as obtained from a least-squares-fitting procedure are listed in Table I. Again the coefficient β_0 has been normalized to unity. The best fit requires a polynomial of $\cos^{2\alpha}\theta$ with α up to and including 3 for both distributions. The value of the coefficients $\beta_{2\alpha}$ resulting from this fit, however, show large uncertainties which can be traced to the sensitivity of the fit to certain data points, notably around 70°, where a slight hump seems to exist. Thus not only do these coefficients show average values quite different from the theoretical ones—also shown in Table I—but more serious is the uncertainty involved. Because of this uncertainty, agreement or disagreement with theory cannot be decided at this point. Taking additionally into account, however, the visual difference between experimental and theoretical curves, we must conclude that some unknown (for the time being) influence prevents quantitative agreement. The possibility of hyperfine coupling during the laser pulse may be partly responsible for this discrepancy. Also, the small contribution of nonresonant purely dipole three-photon ionization (which is estimated to be no more than 5%) may play some role from 70° to 110°, where the PAD of the quadrupole signal drops to small values. There is thus a number of questions raised by this work that will occupy us in a following paper.

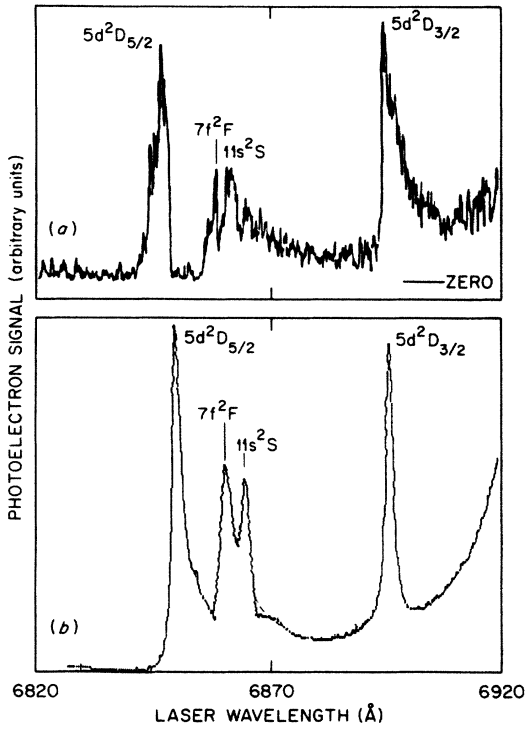

FIG. 6. Ionization signals as a function of wavelength showing the one-photon resonant, two-photon ionization signals due to the quadrupole allowed $5d\,^2D_{5/2,3/2}$ states. Other resonances shown are due to three-photon ionization with enhancement occurring at the two-photon level. (a) Experimental results and (b) calculation.

V. CONCLUSIONS

This paper reports detailed experimental and theoretical studies of MPI and PAD resonantly enhanced by quadrupole transitions. Both theory and experiment show that when the electrons are analyzed perpendicular to the light propagation direction ($\phi=0$), the angular distributions are independent of the fine-structure level excited. The theory also adequately reproduces the qualitative features of the data. Small deviations between experiment and theory are attributed to dipole-dipole contributions and the effects of hyperfine coupling at the intermediate level due to the long temporal profile of the laser pulse.

Measurements of the ratio of two-photon ionization yield for circularly to linearly polarized light via the $6d\,^2D_{5/2,3/2}$ quadrupole resonance are also compared to theoretical calculations. Difficulties with previous experiment and theory are addressed.

ACKNOWLEDGMENTS

The research was sponsored by the Office of Health and Environmental Research, U.S. Department of Energy under Contract DE-AC05-84OR21400 with the Martin Marietta Energy Systems, Inc. This work was supported in part by National Science Foundation Grant No. PHY-86-09966 and in part by DOE Grant No. DE-FG03-87ER60504.

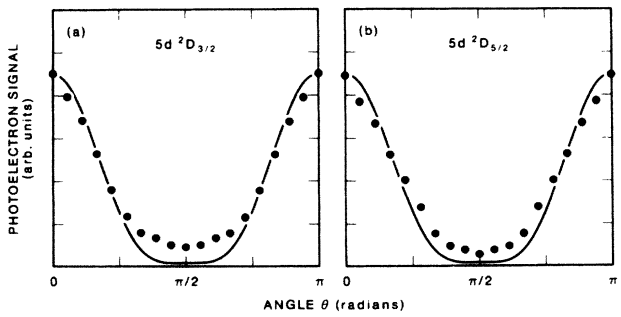

FIG. 7. Photoelectron angular distributions for one-photon resonant, three-photon ionization via the (a) $6s\,^2S_{1/2}\rightarrow 5d\,^2D_{3/2}$ and (b) $6s\,^2S_{1/2}\rightarrow 6d\,^2D_{5/2}$ transitions in cesium atoms. The dots are experimental values and the solid lines represent the theory. Standard deviations in the experimental data are approximately twice the diameter of the dots.

APPENDIX

Calculation of the hfs energy spacing and corresponding coupling times is the following:

$$W_F = 1/2h\,AK + hB\frac{\frac{3}{2}K(K+1)-2I(I+1)J(J+1)}{2I(2I-1)2J(2J-1)},$$

$$K = F(F+1)-I(I+1)-J(J+1).$$

For Cs, $I=7/2$, and we have for $6\,^2D_{3/2}$,

$$F=2,5, \quad A=16.30 \text{ MHz}, \quad |B|<8 \text{ MHz},$$

and for $6\,^2D_{5/2}$,

$$F=1,6, \quad A=-3.6 \text{ MHz}, \quad B=0.$$

In case (i) we have for $6D_{3/2}$,

$$F=2, \quad K=-\tfrac{27}{2},$$

$$W_2=-\tfrac{27}{4}A \quad (\text{assuming } B=0),$$

and for $6D_{3/2}$,

$$F=5, \quad K=\tfrac{21}{2},$$

$$W_2=\tfrac{21}{4}A \quad (\text{assuming } B=0),$$

$$\Delta W_F = W_5 - W_2 = 12A = 195.6 \text{ MHz}.$$

If we assume $|B|=8$ MHz, there is a correction ± 2 MHz, we have in case (ii) for $6D_{5/2}$,

$$F=1, \quad K=-\tfrac{45}{2},$$

$$W_1=\tfrac{1}{2}(-3.6)(-\tfrac{45}{2})=40.5 \text{ MHz},$$

and for $6D_{5/2}$,

$$F=6, \quad K=\tfrac{35}{2},$$

$$W_6=\tfrac{1}{2}(-3.6)(\tfrac{35}{2})=-31.5 \text{ MHz},$$

$$|\Delta W_F|=72 \text{ MHz}.$$

The corresponding coupling times follow for $6D_{3/2}$,

$$F=2,5, \quad \tau_{\text{hfs}}=5.112 \text{ ns},$$

and for $6D_{5/2}$,

$$F=1,6, \quad \tau_{\text{hfs}}=13.89 \text{ ns}.$$

---

*Also at Department of Physics and Research Center of Crete, University of Crete, Iraklion, Crete, Greece.

†Also at Physics Department, Auburn University, Auburn, Alabama 36830. Present address: Max-Planck-Institut für Quantenoptik, Garching, Federal Republic of Germany.

‡Permanent address: Department of Physics, Ripon College, Ripon, WI 54971.

§Also at Chemistry Department, University of Tennessee, Knoxville, TN 37996.

[1]P. Lambropoulos, G. Doolen, and S. P. Rountree, Phys. Rev. Lett. **34**, 636 (1975).

[2]M. Lambropoulos, S. E. Moody, S. J. Smith, and W. C. Lineberger, Phys. Rev. Lett. **35**, 159 (1975).

[3]H. Kaminsky, J. Kessler, and K. J. Kollath, J. Phys. B **12**, L383 (1979).

[4]M. Jaouen, A. Declemy, A. Rachman, and G. Laplanche, J. Phys. B **13**, L699 (1980).

[5]A. Rachman, G. Laplanche, Y. Flank, and M. Jaouen, Phys. Lett. **58A**, 155 (1976).

[6]A. Rachman, G. Laplanche, Y. Flank, and M. Jaouen, J. Phys. (Paris) **38**, 1243 (1977).

[7]G. Leuchs, S. J. Smith, S. H. Dixit, and P. Lambropoulos, Phys. Rev. Lett. **56**, 708 (1986); A. Dodhy, R. N. Compton, and J. A. D. Stockdale, Phys. Rev. A **33**, 2167 (1986).

[8]R. N. Compton, J. A. D. Stockdale, C. D. Cooper, X. Tang, and P. Lambropoulos, Phys. Rev. A **30**, 1766 (1984); W. Christian, R. N. Compton, J. A. D. Stockdale, J. C. Miller, C. D. Cooper, X. Tang, and P. Lambropoulos, *ibid.* **30**, 1775 (1984); A. Dodhy, J. A. D. Stockdale, R. N. Compton, X. Tang, P. Lambropoulos, and A. Lyras, *ibid.* **35**, 2878 (1987).

[9]S. M. Hamadani, J. A. D. Stockdale, R. N. Compton, and M. S. Pindzola, Phys. Rev. A **34**, 1938 (1986).

[10]C. E. Klots and R. N. Compton, in *Multiphoton Processes*, edited by P. Lambropoulos and S. J. Smith (Springer-Verlag, Berlin, 1984), p. 58.

[11]P. Lambropoulos, Adv. At. Mol. Phys. **12**, 87 (1976).

[12]S. N. Dixit and P. Lambropoulos, Phys. Rev. A **27**, 861 (1983).

[13]A. Z. Msezane and S. T. Manson, Phys. Rev. Lett. **35**, 364 (1975); *ibid.* **48**, 473 (1982); Phys. Rev. A **29**, 1594 (1984); I. B. Goldberg and R. H. Pratt, *ibid.* **36**, 2108 (1987).

[14]See, for example, G. Baum, M. S. Lubell, and W. Raith, Phys. Rev. A **5**, 1073 (1972).

[15]P. Lambropoulos and X. Tang, Phys. Rev. Lett. **56**, 401 (1986).

[16]Calculated from data given in E. Arimondo, M. Inguscio, and P. Violino, Rev. Mod. Phys. **49**, 31 (1977).